VOL. 11, NO. 24, DECEMBER 2016 ISSN 1819-6608
ARPN Journal of Engineering and Applied Sciences

www.arpnjournals.com

AN OPTIMAL PARAMETER EXTRACTION AND CRACK IDENTIFICATION METHOD FOR SOLAR PHOTOVOLTAIC MODULES

Chellaswamy C.[1] and Ramesh R.[2]
[1]Rajalakshmi Institute of Technology, Department of Electronics and Communication Engineering, St. Peter's University, Chennai, India
[2]Department of Electronics and Communication Engineering, Saveetha Engineering College, Chennai, India
E-Mail: chellaswamy.c@ritchennai.edu.in

ABSTRACT

A novel parameter extraction method based on Adaptive Differential Evolution Technique (ADET) is introduced for various types of solar photovoltaic (PV) modules. Cracks can isolate large portion of a module and increases the electrical resistance, thus current-voltage (I-V) drop will be increased and it leads to power loss. The parameter extraction and crack identification problem is based on the single diode model of a solar cell. The simulation is performed using an objective function for minimizing the difference between the estimated and measured values. The simulation result is compared with the I-V data set showed that the proposed ADET outperforms other techniques such as chaos particle swam optimization (CPSO), genetic algorithm (GA), simulated annealing (SA) and organic and inorganic solar cells (OIS). Finally, the proposed ADET method is practically validated with three different types of solar modules such as thin film, mono-crystalline and multi-crystalline. The performance of different solar cell modules has been verified and the result shows that the proposed method is suitable for parameter extraction of PV modules.

Keywords: parameter extraction, photovoltaic, adaptive differential evolution, solar module, irradiance, crack identification.

1. INTRODUCTION

A renewable energy source such as photovoltaic (PV) and wind energy has significant growth for the last few decades. Renewable sources produce local heat, even though the thermal reduction is achieved by avoiding CO_2 emission. The PV panels are dark and absorbing around 85% of incoming light whereas 15% is used to generate electricity, the remaining 70% will produce heat [1]. In order to collect the performance data, data acquisition system is widely used in hybrid power source applications. A data acquisition card is used to send the received data to the PC. Both the renewable sources are widely used because of its social and environmental benefits. This source will be the important power source for future with government incentives and public support [2]. The possibilities of providing electricity through a renewable hybrid energy system to a remotely located community are proposed by Bekele *et al.* [3, 4]. The hybrid energy system which utilizes wind and solar is a better alternative for stand-alone applications. This type of energy system is implemented in a region Hurghada in Egypt for a reverse osmosis desalination system [5]. For minimizing the life cost, Hafez and Bhattacharya proposed an optimal design of a hybrid energy system which includes PV, wind and a micro-hydro for generating power [6].

Developing suitable models are required to simulate and predict the behavior of PV modules. There are two main models such as single diode and double diode models are used for PV cells and PV modules [7]. The accuracy and number of parameters used to calculate the I-V characteristics of PV module will differ from each models. It is noted that the double diode model is more accurate than single diode model, which is based on solar panel behavior [8]. To evaluate the PV systems, these models should be used with its parameters. The parameters can be extracted in two ways: the first one is fitting the theoretical I-V curve with the experimental data. In the second method, few key points of experimental data have been taken for determining the parameters [9, 10]. The second method is attractive because it needs few data from I-V curves and its speed. It has to be noted that the I-V curve is highly non-linear and the extracted parameters provides errors if wrong points has been selected. However, the curve fitting algorithms requires large computations and the accuracy depends on the cost function, type of algorithm and initial value of the parameters to be extracted [11]. The conversion efficiency of practical solar cell is in the range of 15-20%. To extract the maximum power from the solar PV cells is a challenging job for the researchers to select proper materials and suitable techniques. In commonly used solar cell technology, the electrons are collected on the top of the solar cell by fingers or grid lines which is deposited on the surface of the solar cells. The fingers are connected with two or three busbars which are soldered on the surface of cells are shown in Figure-1. To avoid partial shading provoked by busbars and fingers, a back contact is used and there is no busbars and fingers. In this work, we modeled the solar cells with front contacts.

Cracks can originate during different stages from production to installation of solar cells and it can isolate large portion of a module and increases the electrical resistance between fingers and solar cell contact. Such broken portion contribute drop in the I-V (current-voltage) of the whole module and leads to power loss [12]. It may be invisible but can be identified accurately by electroluminescence method (EM). The probability of cracking occurs in solar cell has been proposed by Sander *et al* [13]. The strength and stress level of silicon solar cells also been studied.

In the past few decades, various parameter extraction methods such as analytical parameter extraction

method [14], non-linear fitting algorithms [15] are used to extract parameters from PV cell models. Optimization and metaheuristics algorithms are widely used in parameter extraction of solar cells. Evolutionary algorithms are the natural choice for parameter extraction problems which are capable to solve other than the standard test condition. Evolution algorithm methods are very attractive to solve parameter extraction regardless of gradient and information of initial conditions [16]. Various evolutionary algorithms such as genetic algorithm (GA) [17, 18], chaos particle swam optimization (CPSO) [19], simulated annealing (SA) [20] have been included in parameter extraction for solar cells. The electrical characteristics of solar cells and parameter extraction using GA are calculated from the maximum power point [21]. The PSO technique is used to extract various parameters of PV module [22, 23]. The modified differential evolution algorithm called penalty based DE algorithm is used to extract various parameters of solar cells [24].

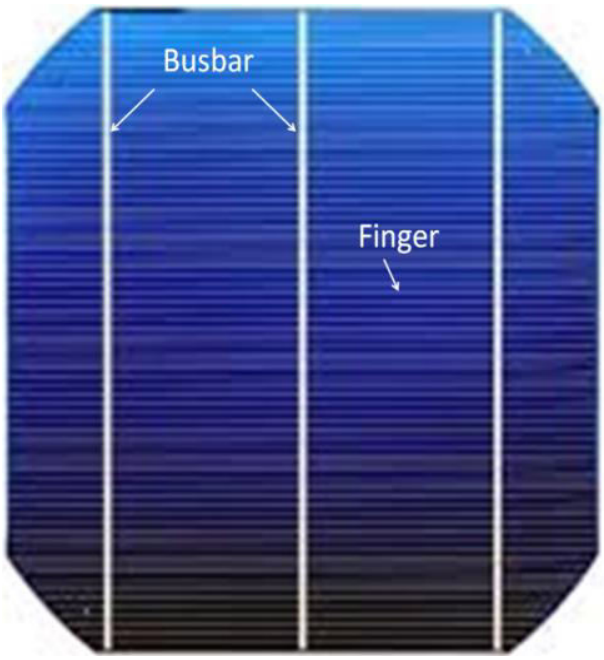

Figure-1. The solar cell showing fingers and busbars with two cracks.

GA has limitations like low speed and degradation [25]. The trade-off between temperature, cooling schedule and inconsistencies are the major issue to make SA less choice for parameter extraction problems [26]. To improve the consistency of the estimation, PSO is introduced in conjunction with cluster analysis. The PSO is used to estimate the parameters and the cluster analysis for filtering the non-feasible solution [27, 28]. It increases the consistency and reliability, even though it requires all previous points to be stored. It increases the computational burden and hence the simulation speed will be greatly affected. The searching space of parameters should be broadened to avoid convergence problems and the extraction processes satisfy different boundary conditions. The V-I characteristics of organic and inorganic solar cells (OIS) studied by Chegaar *et al.* [29]. Various parameters of solar cells are extracted and the energy conversion and management also studied. A maximum power point tracking (MPPT) of solar PV modules for fast varying solar radiations model has been tested in ANFIS-based MPPT control scheme. Various parameters of solar module have been studied by El-Naggar *et al.* [30] using SA algorithm. Unlike conventional differential evolution (DE), the solution of adaptive DE is always in the feasible region and unconstrained in nature. This is where the inclusion of adaptive DE. As a result, more number of solutions will be created. The solutions take part in the evolution process and the accuracy, where diversity and consistency will be improved. In this work, the performance of ADET is investigated for a solar module parameter extraction process and compared with four other methods namely GA, CPSO, SA and OIS. The crack identification model has been introduced and the result is verified by both the experimental and numerical. The remainder of this paper is organized in the following ways: section 2 describes the problem formulation of parameter extraction with double diode model and parameter dependent on temperature and irradiance levels; section 3 describes the DE and adaptive DE algorithm; section 4 explains the simulation and experimental results; and finally, conclusion is discussed in section 5.

2. PROBLEM FORMULATION

The main objective of the parameter extraction for solar cell models is to minimize the difference between measured and simulated current. Two circuit models (single and double diode) are familiarly used to describe the performance of solar cells. The single diode model provides better performance under normal operating condition but the performance is very less at low irradiance [31]. On the other hand, the two diode model [32] modifies the current equation by including the recombination losses in space-charges by incorporating an additional diode.

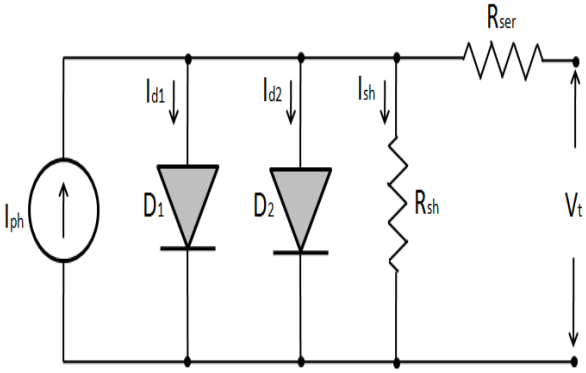

Figure-2. Equivalent circuit model of solar cell using double diode model.

a) Double diode model

The equivalent circuit model of solar cell using double diode model is shown in Figure-2. In this model, the terminal current I_t can be represented as follows [33-35]:

$$I_t = I_{ph} - I_{sd1} - I_{sd2} - I_{sh} \quad (1)$$

$$I_t = I_{ph} - I_{sd1}\left[exp\left(\frac{q(V_{pv}+R_{ser}I_{pv})}{m_{i1}N_sKT_j}\right)-1\right] - I_{sd2}\left[exp\left(\frac{q(V_{pv}+R_{ser}I_{pv})}{m_{i2}N_sKT_j}\right)-1\right] - \left(\frac{V_{pv}+R_{ser}I_{pv}}{R_{sh}}\right) \quad (2)$$

Where q represents the charge of electron ($1.6x10^{-19}$ C), I_{ph} represents the photovoltaic current, K represents the Boltzmann constant ($1.38x10^{-23}$ J/K), I_{ph} is the cell-generated photocurrent, N is the number of module serially connected, T_j is the junction temperature of the module, I_{ph} is the photovoltaic current. The subscript 1 and 2 represents first and second diode respectively. Seven parameters such as series resistance (R_{ser}), shunt resistance (R_{sh}), saturation current of diodes (I_{sd1} and I_{sd2}) and ideality factor (m_{i1} and m_{i2}) of diode can be extracted from the given set of I-V data.

b) Parameters dependence on temperature and irradiation levels

The standard test conditions (STC) can be referred from the manufacturer's catalogue and the parameters recognized from the datasheet are applicable only under STC. The dependence of the parameters on the temperature and irradiance levels is determined using the principle of supervision [36,37]. The dependence of the PV model parameters can be inserted and the I-V relationship can be realized. In this paper, the parameters such as R_{ser}, R_{sh}, I_{sd1} and I_{sd2} are used the similar relation utilized in [36] and [38].

$$R_{ser} = R_{STC} \quad (3)$$

$$R_{sh} = R_{sh,STC} \quad (4)$$

$$\frac{I_{sd1}}{I_{sd1,STC}} = \left[\frac{T}{T_{STC}}\right]^3 e^{\left[\frac{1}{K}\left(\frac{B_{g,STC}}{T_{STC}}-\frac{B_g}{T}\right)\right]} \quad (5)$$

The value of band gap energy B_g, in T_{STC}=25° C is set to 1.121 eV for silicon cells [36], [38]. B_g can be expressed in terms of cell temperature according to [37], [38] is given by

$$\frac{B_g}{B_{g,STC}} = 1 - 0.0002677(T - T_{STC}) \quad (6)$$

The photo current on the irradiation level and temperature can be expressed as [35]:

$$\frac{I_{ph}}{I_{ph,STC}} = \frac{B_g}{B_{g,STC}}[1 + T_{sh}(T - T_{STC})] \quad (7)$$

where the temperature coefficient of the short circuit current T_{sh}, is (%/°C). The parameter I_{sd2} as a function of cell temperature can be expressed as:

$$I_{sd2} \propto T^{\frac{5}{2}} e^{\left(-\frac{B_g}{2KT}\right)} \quad (8)$$

Now (8) can be written by introducing proportionality constant C as:

$$I_{sd2} = C\,T^{\frac{5}{2}} e^{\left(-\frac{B_g}{2KT}\right)} \quad (9)$$

Now (9) can be evaluated at STC and after reducing with some algebra, we can get

$$\frac{I_{sd2}}{I_{sd2,STC}} = \left[\frac{T}{T_{STC}}\right]^{\frac{5}{2}} e^{\left[\frac{1}{2k}\left(\frac{B_{g,STC}}{T_{STC}}-\frac{B_g}{T}\right)\right]} \quad (10)$$

The parameters in (3), (4), (5), (7) and (10) can be applied into (2) to extract the I-V characteristics of PV module at different operating conditions.

c) Crack identification model

The most common PV cells are made of silicon and the fingers (metal grids) are present in the top layer and the electrical contacts made by metal bases on the bottom of the cell. The fingers are soldered to busbars and they are connected in series with different solar cells to form the PV module is shown in Figure-1. The homogeneous properties of the solar cell, the current flow $I_F(\beta)$ along the finger can be determined by a one-dimensional electric model and the value of β described by each position varies from one busbar to other. The voltage is a function of β due to distributed resistance (metallization and emitter resistance) of the grid line [39]. For each voltage V(β), the surface current density, I_t can be determined using single diode model. The finger crossed by a crack has been verified but the relation between the localized resistance and crack opening are not investigated by Berardone *et al* [40]. This problem has been included in the present work.

The electroluminescence test is carried out under no direct illumination from the sun instead it is performed inside a dark room with externally applied by a power supply through busbars. The current density along the finger $I_F(\beta)$ can be represented by the differential equation as:

$$\frac{dV(\beta)}{d\beta} = - R_S I_F(\beta) \quad (11)$$

where R_s represents the sheet resistance in the β direction. The current density passing through the solar cell is equal to the derivative of current density along the finger and it can be represented as:

$$\frac{dI_F(\beta)}{d\beta} = - I_t(\beta) \quad (12)$$

Substitute Equation. (11) into Equation. (12), it will produce the following second order differential equation as:

$$\frac{d^2V(\beta)}{d\beta^2} = R_S I_t(\beta) \quad (13)$$

The response of current density through the thickness of the solar cell can be determined by a single diode model [41]:

$$I_t(\beta) = I_0 \exp\left(\frac{V(\beta) - R_{sd} I_t}{mV_T}\right) \quad (14)$$

where I_0 is the saturation current density, R_{sd} represents the sheet resistance in series with the diode, m is ideality factor of diode, and the thermal voltage, $V_T = kT/e$. k is Boltzmann constant, T is temperature, and e is charge of electron. Now apply Newton-Raphson method on Equation. (14) and it can be written as:

$$f(I_t(\beta)) = I_t(\beta) - I_0 \exp\left(\frac{V(\beta) - R_{sd} I_t}{mV_T}\right) = 0 \quad (15)$$

d) Solar cell model optimization problem

The solar cell model parameter extraction is an optimization process which minimizes the difference between real and estimated values. The parameter estimation using optimization technique implemented in the following approach:

- A set of real data of I-V for a PV module is measured.
- Defined an objective function for minimizing the difference between the real data and measured values.
- Tune the parameters by applying an optimization algorithm until the best objective function obtained.
- After completing the optimization algorithm, the optimal value is extracted from the solution obtained by the optimization algorithm.

Now assign a vector U, for each value which is extracted from the optimization algorithm. The vector for double diode model is U= [R_s, R_{sh}, I_{sh}, I_{sd1}, I_{sd2} m_{i1}, m_{i1}, $I_t(\beta)$]. An objective function needs to be defined in the optimization problem and the corresponding function for solar model parameter extraction can be defined from (2). The homogeneous equations for the corresponding equations are given as:

$$f(V_t, I_t, U) = I_t - I_{ph} + I_{sd1}\left[\exp\left(\frac{q(V_{pv}+R_{ser}I_{pv})}{m_{i1}N_sKT_j}\right) - 1\right] + I_{sd2}\left[\exp\left(\frac{q(V_{pv}+R_{ser}I_{pv})}{m_{i2}N_sKT_j}\right) - 1\right] + \left(\frac{V_{pv}+R_{ser}I_{pv}}{R_{sh}}\right) \quad (16)$$

Now the values of U can be put into (16), the solution of f (V_t, I_t, U) for each pair of V-I data can be measured. The difference between real and estimated data can be evaluated, typically by the root mean square error (RMSE) criterion. For parameter extraction of solar cell models the following objective function is used to minimize the RMSE as:

$$minimize\ RMSE\ (B) = \sqrt{\frac{1}{M}\sum_{i=1}^{M} f(V_t, I_t, U)^2} \quad (17)$$

where M is the number of real V-I data and the output of RMSE guide the optimization search for better value of the vector U. If the value of RMSE is bad, the optimization algorithm tuned the vector U and send back to (16). This iterative procedure improves the value of vector U and stopped if the output value is good enough or the optimization algorithm attains maximum iteration time.

3. DIFFERENTIAL EVOLUTION ALGORITHM

Differential evolution is a heuristic, population based algorithm originally proposed by Storn and Price in 1997 [42]. DE is a search and optimization technique which generates new vectors by adding the third one with the difference of two population vectors. There are several variants of DE and it can be expressed as:

$$DE/mu/dv/cr \quad (18)$$

where mu, dv and cr represents the mutated vector, number of difference vector and crossover scheme respectively. DE has different advantages such as simple, robust, few control parameters and effective. It can also work with multi-dimensional, noisy and time dependent objective functions [43]. Based on these advantages, we choose DE for optimization parameter estimation problem.

a) DE-Based optimal parameter estimation

Consider the solar cell model parameter optimization as (17), U is the decision variable which contains n variables $x_i \epsilon R^n$. The step by step procedure for implementing DE algorithm is described as follows:

step 1. The population (NP) of D-dimensional parameter vector U_i^k and the population of solution P^k, $P_u^k = U_i^k$, i=1,2,...,NP; k=1,2,...,k_{max} and $U_i^k = U_{j,i}^k$, j=1,2,...,D.

The index, i represent the population index, j represents the parameters within the vectors and k is the generation to which a vector belongs.

The population NP has D-dimensional vectors$U_i^k = [U_{1,i}^k, U_{2,i}^k, \dots, U_{j,i}^k, \dots, U_{D,i}^k]$. Each vector forms a candidate solution to the D-dimensional optimization problem and values are randomly selected within the interval U_L and U_M. $U_L = [U_{1,L}, U_{2,L}, \dots, U_{D,L}]$and $U_M = [U_{1,M}, U_{2,M}, \dots, U_{D,M}]$ are the lower and upper limits of the search space. Now the initial population in the search space by:

$$U_{j,i}^1 = U_L + rand[1](U_M - U_L) \quad (19)$$

The solution of parameter estimation is feasible because they are initialized within the feasible range and we have to find the optimal one.

step 2. According to (17) evaluate the fitness of each individual in the population.

step 3. Create new population by:

(1) Mutation: For the given parameter vector U_i^k, randomly choose three different vectors $(U_r^k, U_{r2}^k, U_{r3}^k)$ in the range [1, NP]. A trial vector $V_i^k$is created by adding the third vector to the difference between the two vectors and is given by

$$V_i^k = U_{r1}^k + F(U_{r2}^k - U_{r3}^k) \quad (20)$$

where F is the mutation scaling factor having range (0,1).

(2) Crossover: The trial vector V_i^{k+1} and the target vector U_i^k are mixed to yield a new vector as:

$$Y_i^k = [Y_{1i}^k, Y_{2i}^k, \dots, Y_{ji}^k, \dots, Y_{Di}^k] \quad (21)$$

In this work, binomial crossover strategy [35] is used and it can be expressed as:

$$Y_{j,i}^k = \begin{cases} V_{j,i}^k, & if(rand \le RC) \\ U_{j,i}^k, & otherwise \end{cases} \quad (22)$$

where RC is the rate of crossover.

(3) Selection: For each $U_{j,i}$ and corresponding $Y_{j,i}$ to select next generation vector, k=k+1 as:

$$U_i^{k+1} = \begin{cases} Y_i^k, & if\ J(Y_i^k) < J(U_i^k) \\ U_i^k, & otherwise \end{cases} \quad (23)$$

where J(U) is the objective function to be minimized. Thus, the new trial vector swaps its values with the target; if objective function value is less otherwise the target is conserved in the population.

b) Adaptive DE algorithm

The parameter setting in DE is crucial [44, 45] and to overcome this drawback by Zhang and Sanderson introduces an adaptive DE algorithm [46, 47]. The parameters P^k, F and RC are adaptively control and generate the parameters successfully. The adaptation is described as follows:

(1) Mutation factor adaption: Each individuals U_i^k and associated individuals are mutated with the mutation rate M_r and obtained by the strategy DE/mu/dv/cr [44] as follows:

A trial vector $V_i^k$is created by adding the third vector to the difference between the two vectors and is given by

$$V_i^k = U_{r1}^k + F(U_{r2}^k - U_{r3}^k) \quad (24)$$

where F is the mutation scaling factor having range (0,1) and is given by

$$F_i^{k+1} = \begin{cases} 1 - rand_1^{\left(1-\frac{k}{k_{max}}\right)^b}, & if\ rand_2 < M_r \\ F_i^k, & otherwise \end{cases} \quad (25)$$

where k is the current generation, k_{max} is the maximum generation, and $rand_1$ and $rand_2$ are the uniform random values within the range (0,1). The scaling factor F, should be adaptive with the following mutation rate M_r and is determined as:

$$M_r = \frac{f(U_i^k) - min(f(U_i^k))}{max(f(U_i^k)) - min(f(U_i^k))} \quad (26)$$

f(.) is the objective function.

(2) Crossover adaptation: The crossover rate RC_i is independently calculated for each vector as:

$$RC_i = rndn_i(P_{RC}^k, 0.1) \quad (27)$$

where P_{RC}^k is the mean value to generate RC_i. It is updated as:

$$P_{RC} = (1 - q)P_{RC} + q\ mean_A(S_{RC}) \quad (28)$$

where q is a constant in the range (0,1), S_{RC} is the set of successful rate of RC_i and $mean_A(.)$ is the usual arithmetic mean operation.

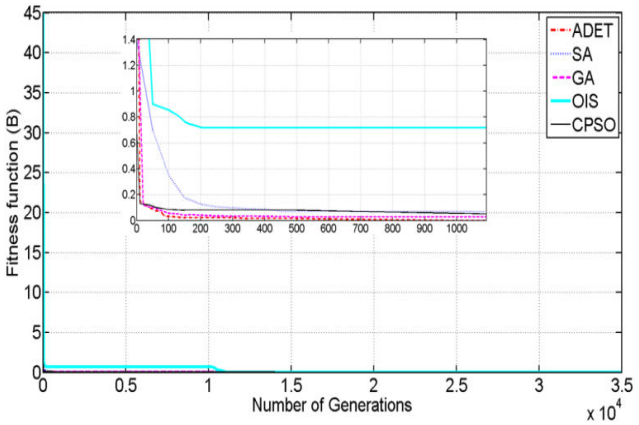

Figure-3. Convergence performance of ADET and various other methods during parameter extraction.

4. SIMULATION AND EXPERIMENTAL RESULTS

In this section, the parameters of ADET have been studied by using measured data. The measured voltage and current data of solar cell and PV module are taken in this simulation. The prototype of PV module has 39 polycrystalline silicon are connected in series, totally 1200 W/m^2 and the voltage and current are measured under one sun at 33^o C. Various parameters of ADET used in this simulation are as follows: the population size NP=150, maximum number of generation k_{max}=500, Length of individual L_i=3, DE-step size S=0.5, merging generation rate P_m=0.5, crossover probability constant C_r=0.5 and the termination criteria T_c =1 x e^{-6}.

a) Simulation results

The prototype of PV module has 39 polycrystalline silicon are connected in series, totally 1200 W/m^2 and the voltage and current are measured under 1 sun at 33^o C. Here the real values of voltage and current of PV module is same as [48]. The extracted parameter values and the RMSE obtained by the proposed method and other four algorithms are presented in Table-1. The proposed ADET method is compared with other parameter extraction techniques such as CPSO, GA, OIS and SA. It is seen that, the ADET has lowest RMSE compared to other parameter extraction techniques such as CPSO, GA, SA and OIS. Since ADET has lowest RMSE, we conclude that the performance of ADET is very good and it is suitable for parameter extraction in solar cells. The relative error (RE) and individual absolute error (IAE) are used to show the performance of parameter extraction methods [43] and it can be defined as:

$$IAE = |I_m - I_e| \quad (29)$$

$$RE = \frac{|I_m - I_e|}{I_m} \quad (30)$$

Table-1. Comparison of RMSE for various parameter extraction methods with proposed ADET.

Parameters	CPSO	GA	OIS	SA	ADET
Iph (A)	3.1254	3.33166	3.13674	3.2334	3.43045
Isd1 (A)	$5.0743x10^{-6}$	$4.3731x10^{-6}$	$7.1946x10^{-7}$	$5.6387x10^{-8}$	$3.31089x10^{-6}$
Isd2 (A)	$0.329x10^{-5}$	$2.742x10^{-5}$	$3.953x10^{-7}$	$4.835x10^{-8}$	$0.254x10^{-6}$
m_1	5.237	4.5832	6.0435	7.7934	3.4379
m_2	5.935	3.684	5.8535	6.0647	3.6943
Rser (Ω)	0.3735	0.30134	0.32897	0.42042	0.31063
Rsh (Ω)	200.100	199.463	203.58	207.5233	200.647
RMSE	0.03521	0.0227	0.04783	0.0385	0.02131
Time (s)	115	335	412	316	44

Additionally, computational speed of all the extraction method is compared with the proposed method. From Table-1 one can easily understand that the ADET method is faster than other parameter extraction methods and it takes 44 seconds to compute various parameters for 30,000 generations. The computational time of CPSO requires around three times greater than ADET. However, the computational time required for GA, OIS and SA are much greater than that of ADET for the same generation. It is noted that CPSO is not converge with the desired solution if lower number of generations are used. On the other hand, ADET consistently converges for both the lower and higher generation levels. This better computational speed is useful to make the proposed method as PV simulator.

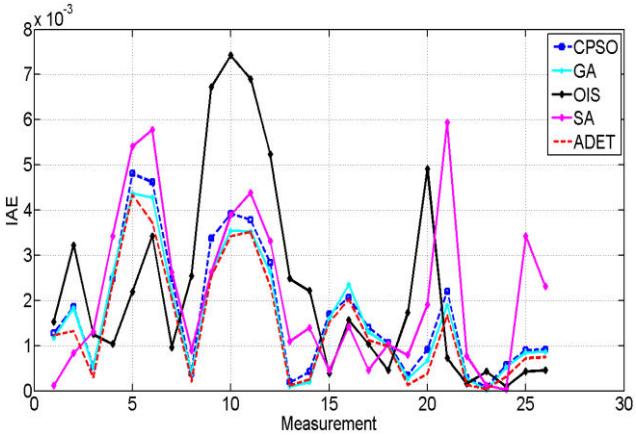

Figure-4. Optimal values of IAE extracted by CPSO, GA, SA, OIS and ADET for the PV module.

The qualitative representation of the convergence performance of ADET and all other methods are shown in Figure-3. The evolution process becomes very slow after 200 iteration according to GA and OIS. It implies that these methods prematurely converges to a local minima at B=0.03. Table-2 also shows that the mean, maximum and minimum values of B are in the order of 10^{-2}. According to CPSO and SA the B_{min} values are close to the threshold

value and the B_{max} is far from the threshold value. It leads to poor standard deviation. On the other hand, Figure-3 illustrate that the exploration capability of both the CPSO and SA are not efficient and their RMSE languish after 15,000 generations. In contrast, the ADET shows that it has very low RMSE and provides high accuracy. The zoomed view is shown inside the Figure-3. From the zoomed view one can clearly understand that the RMSE of ADET has been improved up to around 500 iterations and it settled with the mean value of 2.873×10^{-9}. The standard deviation of ADET is very small and almost it is negligible which indicates that the solution obtained by every run is highly consistent.

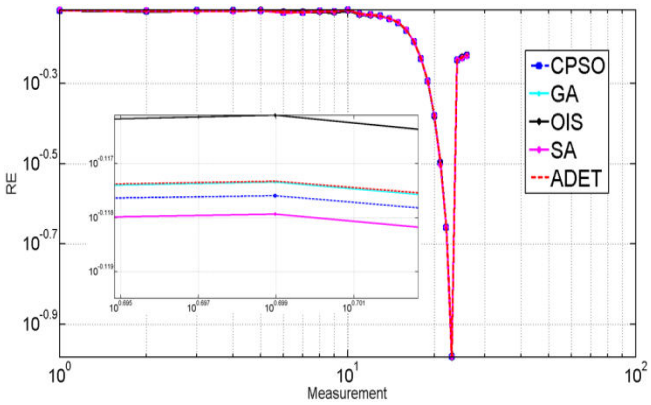

Figure-5. Relative error estimated by CPSO, GA, SA, OIS and ADET.

The optimal value of IAE for each measurement using ADET and other parameter extraction techniques such as CPSO, GA, SA and OIS are presented in Table-3. The comparison between CPSO, GA, SA, OIS and the proposed method with the optimal value of IAE for each measurement is illustrated in Figure-4. From Figure-4 one can easily understand that the ADET method has better performance than other parameter extraction methods such as CPSO, GA, SA, and OIS. The total IAE values for each measurement is also calculated and presented in the Table-3. The total IAE value of table 3 point out that the ADET has lowest total IAE compared to other methods for the PV module. From Table-3 and Figure-4 one can easily understand that ADET outperforms CPSO, GA, SA, and OIS for this parameter extraction problem. Figure-5 illustrate that the comparison between CPSO, GA, SA, OIS and the proposed method with the optimal value of RE for each measurement. The IAE of the proposed method is very low compared to other parameter estimation techniques. On the other hand the value of RE is in between CPSO and OIS. The zoomed view is shown inside the Figure-5. From the zoomed view one can clearly understand that the deviation is very little compared to other method. From the result we observed that the values extracted by ADET in the PV module fit the real data very well. The excellent performance of ADET can be characterized to different factors such as: 1) the diversity of parameter search space can be increased by F and RC; as a result new set of children is generated. 2) An inherent capability of the adaptation process provides guarantees that the parameters are always in the feasible region only. 3) The one-to-one selection ensures that the winning parameters are allowed to take part in the next generation and the parameter which loses even a single competition is eliminated. Generally, these factors provide rapid convergence, highly accurate and consistent solutions. Figure-6 illustrates the V-I characteristics of optimal values extracted by ADET along with the real data. From the result we observed that the double diode model is the best choice for the real data.

Table-2. Optimal values of IAE extracted by CPSO, GA, OIS, SA and ADET for the PV module.

Methods	RMSE min	RMSE max	RMSE mean	σ
CPSO	5.1732×10^{-6}	1.8462×10^{-2}	4.2638×10^{-3}	7.8245×10^{-3}
GA	2.0793×10^{-2}	3.3731×10^{-2}	3.1346×10^{-2}	4.6367×10^{-3}
OIS	5.0743×10^{-5}	2.1043×10^{-4}	1.1043×10^{-4}	5.4301×10^{-5}
SA	5.5893×10^{-5}	2.7353×10^{-4}	1.3941×10^{-4}	6.2843×10^{-5}
ADET	2.8743×10^{-9}	2.8743×10^{-9}	2.8743×10^{-9}	4.6483×10^{-20}

The predicted data of current through the thickness of solar cell with solid line is compared with the experimental data (in blue dot) is shown in Figure-7. The crack opening present in the solar panel under test is: 0.12, 0.18, and 0.23µm for the mid-span deflections 4, 7, 10, and 13 cm respectively. The parameters which are determined from the model for the corresponding solar panel for finger not crossed by crack are: R_s=0.2Ωcm^2, V_T =24mV, R_{ser}=o.12Ω, I_t= $1.43\text{x}10^{-12}$ A/cm^2. The point of finger crossed by the crack can be identified by EM test. The values extracted by ADET are listed in Table-4.

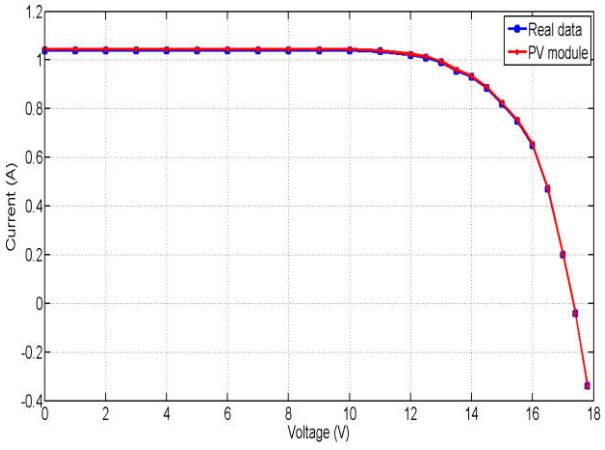

Figure-6. Comparison results of PV module with the real data.

Table-3. Optimal values of IAE extracted by CPSO, GA, OIS, SA and ADET for a PV module.

Im (A)	CPSO			GA			OIS			SA			ADET		
	Ie (A)	IAE	RE	Ie (A)	IAE	RE	Ie (A)	IAE	RE	Ie (A)	IAE	RE	Ie (A)	IAE	RE
0.7640	0.7627	0.00128	0.0017	0.7628	0.00117	0.0015	0.7625	0.00152	0.0020	0.7639	0.00011	0.0001	0.7628	0.00123	0.0016
0.7620	0.7601	0.00186	0.0024	0.7602	0.00184	0.0024	0.7588	0.00322	0.0042	0.7612	0.00083	0.0011	0.7607	0.00132	0.0017
0.7615	0.7610	0.00054	0.0007	0.7610	0.00052	0.0007	0.7602	0.00125	0.0016	0.7602	0.00131	0.0017	0.7612	0.00030	0.0004
0.7635	0.7610	0.00248	0.0032	0.7609	0.00257	0.0034	0.7625	0.00103	0.0013	0.7601	0.00342	0.0045	0.7611	0.00236	0.0031
0.7676	0.7628	0.00481	0.0063	0.7632	0.00437	0.0057	0.7654	0.00219	0.0029	0.7622	0.00541	0.0070	0.7633	0.00434	0.0057
0.7590	0.7544	0.00462	0.0061	0.7547	0.00428	0.0056	0.7556	0.00342	0.0045	0.7532	0.00578	0.0076	0.7553	0.00372	0.0049
0.7570	0.7545	0.00248	0.0124	0.7549	0.00214	0.0107	0.7561	0.00095	0.0048	0.7544	0.00632	0.0131	0.7550	0.00201	0.010
0.7587	0.7583	0.00039	0.0005	0.7583	0.00037	0.0005	0.7562	0.00254	0.0033	0.7578	0.00089	0.0012	0.7585	0.00021	0.0003
0.7598	0.7564	0.00338	0.0044	0.7572	0.00262	0.0034	0.7531	0.00672	0.0088	0.7572	0.00262	0.0034	0.7573	0.00253	0.0033
0.7685	0.7646	0.00392	0.0051	0.7650	0.00354	0.0046	0.7611	0.00742	0.0097	0.7646	0.00389	0.0051	0.7651	0.00342	0.0045
0.7505	0.7467	0.00379	0.0050	0.7470	0.00353	0.0047	0.7436	0.00690	0.0092	0.7461	0.00438	0.0058	0.7470	0.00352	0.0047
0.7465	0.7437	0.00283	0.0038	0.7439	0.00262	0.0035	0.7413	0.00523	0.0070	0.7432	0.00331	0.0044	0.7442	0.00232	0.0031
0.7385	0.7383	0.00019	0.0003	0.7384	0.00010	0.0001	0.7360	0.00248	0.0034	0.7374	0.00109	0.0015	0.7384	0.00011	0.0001
0.7280	0.7276	0.00042	0.0006	0.7278	0.00019	0.0003	0.7258	0.00221	0.0030	0.7266	0.00139	0.0019	0.7278	0.00025	0.0003
0.7122	0.7105	0.00170	0.0024	0.7106	0.00160	0.0022	0.7118	0.00038	0.0005	0.7118	0.00045	0.0006	0.7107	0.00152	0.0021
0.6821	0.6800	0.00206	0.0030	0.6798	0.00235	0.0034	0.6805	0.00157	0.0023	0.6807	0.00142	0.0021	0.6801	0.00202	0.0030
0.6376	0.6362	0.00140	0.0022	0.6363	0.00130	0.0020	0.6366	0.00103	0.0016	0.6371	0.00046	0.0007	0.6365	0.00112	0.0018
0.5778	0.5767	0.00106	0.0018	0.5768	0.00101	0.0017	0.5773	0.00046	0.0008	0.5768	0.00103	0.0018	0.5768	0.00098	0.0017
0.5076	0.5073	0.00034	0.0007	0.5073	0.00027	0.0005	0.5059	0.00172	0.0034	0.5068	0.00079	0.0016	0.5075	0.00013	0.0003
0.4176	0.4167	0.00091	0.0022	0.4169	0.00067	0.0016	0.4127	0.00491	0.0118	0.4157	0.00190	0.0045	0.4172	0.00038	0.0009
0.3199	0.3177	0.00220	0.0069	0.3180	0.00189	0.0059	0.3192	0.00072	0.0023	0.3140	0.00593	0.0185	0.3182	0.00167	0.0052
0.2198	0.2195	0.00029	0.0013	0.2195	0.00027	0.0012	0.2196	0.00016	0.0007	0.2190	0.00077	0.0035	0.2197	0.00013	0.0006
0.1047	0.1046	0.00009	0.0009	0.1047	0.00002	0.0002	0.1043	0.00042	0.0040	0.1046	0.00012	0.0011	0.1047	0.00004	0.0004
0.5736	0.5730	0.00057	0.0010	0.5731	0.00052	0.0009	0.5735	0.00009	0.0002	0.5736	0.00003	0.0001	0.5733	0.00031	0.0005
0.5833	0.5824	0.00090	0.0015	0.5825	0.00085	0.0015	0.5829	0.00043	0.0007	0.5799	0.00342	0.0059	0.5826	0.00072	0.0012
0.5900	0.5891	0.00092	0.0016	0.5891	0.00085	0.0015	0.5896	0.00045	0.0008	0.5877	0.00231	0.0039	0.5892	0.00075	0.0013
Total		0.0454	15.9089		0.04152	15.9128		0.0594	15.8949		0.0557	15.8986		0.03748	15.9169

b) Experimental test

The parameter extraction methods used for PV modules have been tested with experiments. The experimental data is taken from the manufacture datasheet. Three different modules such as thin film (ST36 and ST40), mono-crystalline (SM55 and SQ150PC) and multi-crystalline (MSX-60 and KC200GT) are used for experiments. The experiment is conducted for five different irradiance levels such as 250 W/m^2, 500 W/m^2, 750 W/m^2, 1000 W/m^2 and 1250 W/m^2 and the data is measured. In order to study the quality of optimal values extracted by ADET, various parameters such as R_{ser}, R_{sh}, I_{ph}, I_{sd1}, I_{sd2}, m_{i1} and m_{i2} are put into (3) and then determined the I-V characteristics of PV module. The I-V characteristics of optimal values extracted by ADET along with the real data for thin film, mono-crystalline and multi-crystalline are illustrated in Figure-8, 9 and 10 respectively.

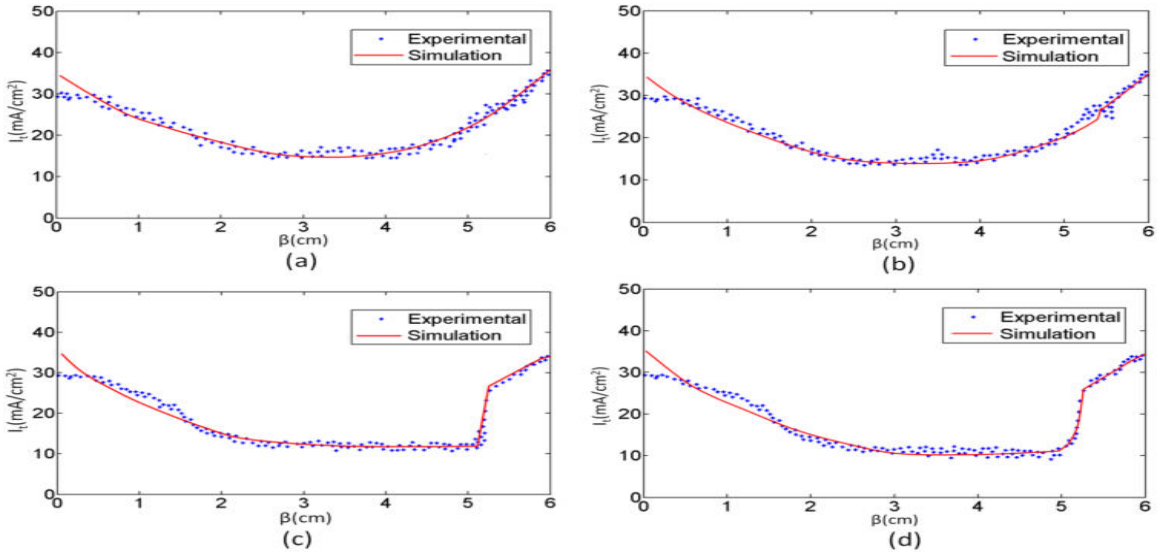

Figure-7. The current I_t in a mono-crystalline Silicon cell along a finger crossed by a crack for four mid-span deflections (a) 4 cm, (b) 7 cm, (10) cm, (13) cm.

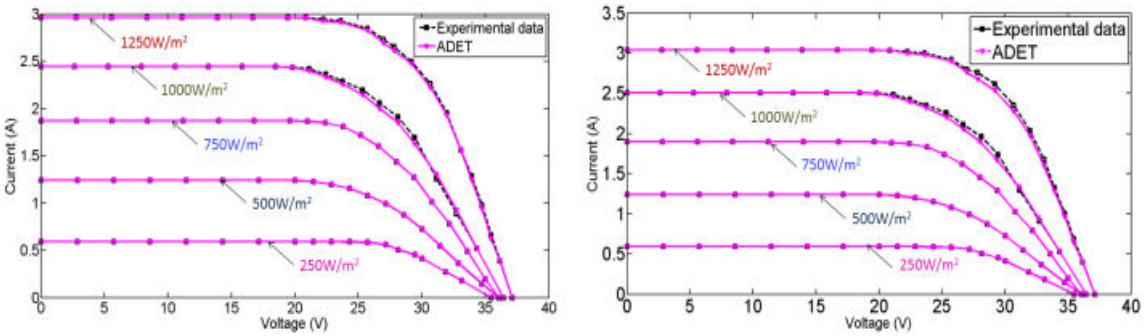

Figure-8. I-V characteristics of thin film solar module using ADET (a) ST36 (b) ST40.

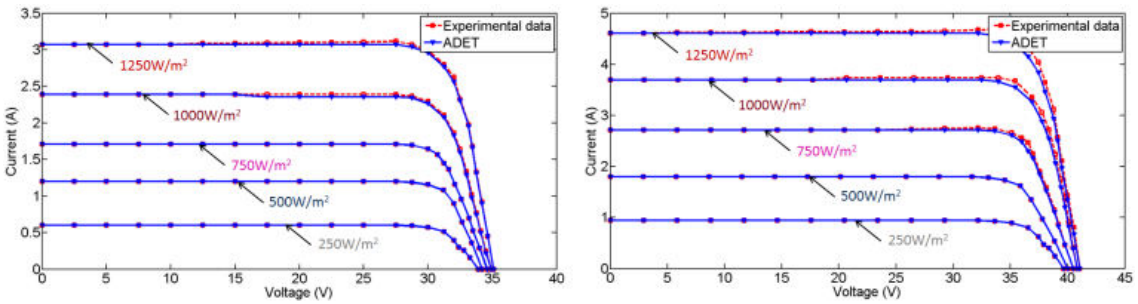

Figure-9. I-V characteristics of mono-crystalline solar module using ADET (a) SQ150PC (b) SM35.

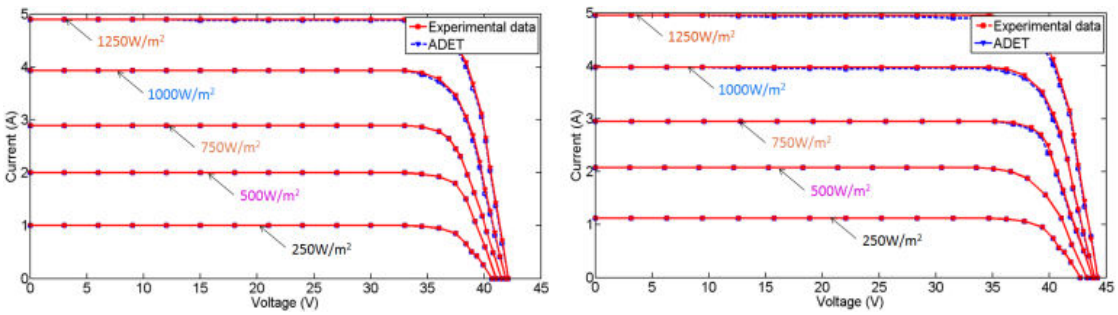

Figure-10. I-V characteristics of multi-crystalline solar module using ADET (a) MSX-60 (b) KG200GT.

From the results one can easily understand that the extracted data is accurately fit with the whole range of experimental data. The accuracy of the result is more in lower irradiances than higher irradiances. The numerical values of the extracted parameters using ADET is shown in Table-5. The experimental results of different solar cell models presented in Table-5 and from the Figure-8-10, the performance of the proposed parameter extraction method verified with good accuracy. From this we conclude that the proposed ADET technique provides good performance in parameter extraction of solar cell models. From the result we observed that the values extracted by ADET in the PV module fit the real data very well. To evaluate the accuracy of ADET, the extracted parameter values are compared to GA which contains minimum RMSE than other parameter extraction methods. Figure-11 shows that the comparison result of three different types of solar modules with different irradiance levels. The proposed method outperforms than other parameter extraction methods and the magnitude of maximum error is less than 0.02. On the other hand, the magnitude of maximum error exceeds more than 0.1 in the case of GA.

Table-4. Parameters extracted by ADET for mono-crystalline solar cell.

Deflection (cm)	β (cm)	V_0(V)	Rs (Ωcm^2)
4	3.823	0.628	0.274
7	3.992	0.634	0.282
10	4.692	0.619	0.318
13	4.976	0.619	0.327

Table-5. Extracted parameters of three solar modules with different irradiance levels.

Parameters	Thin film		Mono-crystalline		Multi-crystalline	
	ST36	ST40	SM55	SQ150PC	MSX-60	KG200GT
k=250 W/m²						
I_{ph} (A)	0.538	0.543	0.689	0.948	0.9737	0.979
I_{sd1} (A)	1.636×10^{-11}	2.784×10^{-7}	4.358×10^{-11}	1.35×10^{-11}	2.264×10^{-8}	6.238×10^{-10}
I_{sd2} (A)	4.472×10^{-5}	5.783×10^{-4}	1.253×10^{-8}	4.439×10^{-8}	5.043×10^{-5}	3.480×10^{-6}
R_{sh} (kΩ)	1258.46	4724.37	351.75	1628.37	320.14	820.34
R_{ser} (Ω)	1.823	0.1023	0.340	0.637	0.136	0.057
m_1	1.918	1.95	1.264	1.924	1.263	1.846
M_2	1.926	2.476	1.748	1.924	2.427	2.637
Time (s)	0.24	0.25	0.25	0.25	0.25	0.26
k=500 W/m²						
I_{ph} (A)	1.599	1.599	1.943	2.693	2.803	2.826
I_{sd1} (A)	4.8×10^{-11}	3.54×10^{-6}	5.286×10^{-10}	4.674×10^{-12}	9.578×10^{-10}	7.26×10^{-8}
I_{sd2} (A)	5.175×10^{-5}	2.472×10^{-5}	2.641×10^{-5}	4.173×10^{-8}	4.681×10^{-5}	3.743×10^{-6}
R_{sh} (kΩ)	809.53	1367.37	409.265	1215.426	403.467	804.536
R_{ser} (Ω)	1.503	0.936	0.704	0.668	0.364	0.052
m_1	1.894	1.486	1.467	1.174	0.946	1.046
m_2	1.894	3.612	2.831	1.325	1.842	2.175
Time (s)	0.27	0.27	0.29	0.29	0.3	0.29
k=750 W/m²						
I_{ph} (A)	1.989	1.984	2.145	2.986	3.357	3.432
I_{sd1} (A)	5.235×10^{-11}	4.836×10^{-6}	6.435×10^{-10}	5.247×10^{-12}	9.265×10^{-10}	3.636×10^{-8}
I_{sd2} (A)	6.385×10^{-5}	4.925×10^{-5}	7.368×10^{-5}	5.035×10^{-8}	7.335×10^{-5}	1.643×10^{-5}
R_{sh} (kΩ)	895.560	1143.635	426.540	1426.634	454.742	627.853
R_{ser} (Ω)	1.47	1.157	0.934	0.742	0.474	0.051
m_1	1.924	1.935	2.250	1.285	0.994	2.289
m_2	2.178	2.358	2.726	2.842	1.745	2.864
Time (s)	0.35	0.34	0.34	0.35	0.37	0.37
k=1000 W/m²						
I_{ph} (A)	2.679	2.703	3.482	4.794	4.724	4.748
I_{sd1} (A)	6.845×10^{-9}	2.225×10^{-8}	2.943×10^{-10}	7.364×10^{-11}	9.631×10^{-9}	7.356×10^{-9}
I_{sd2} (A)	2.753×10^{-5}	2.942×10^{-5}	4.724×10^{-8}	4.083×10^{-8}	2.754×10^{-5}	2.532×10^{-5}
R_{sh} (kΩ)	634.154	248.35	447.35	1583.86	367.25	348.469
R_{ser} (Ω)	1.375	1.295	0.583	0.852	0.258	0.436
m_1	1.745	1.167	2.34	1.272	1.153	1.147
m_2	2.743	1.842	3.742	2.638	2.846	2.864
Time (s)	0.38	0.39	0.37	0.37	0.4	0.39
k=1250 W/m²						
I_{ph} (A)	2.935	2.843	3.746	4.995	5.155	4.993
I_{sd1} (A)	2.983×10^{-9}	2.99×10^{-8}	3.75×10^{-10}	8.465×10^{-11}	9.957×10^{-11}	2.165×10^{-11}
I_{sd2} (A)	2.256×10^{-5}	2.248×10^{-6}	6.245×10^{-6}	6.683×10^{-8}	3.532×10^{-5}	2.942×10^{-8}
R_{sh} (kΩ)	231.643	215.759	486.359	1647.64	324.350	298.427
R_{ser} (Ω)	1.258	1.437	0.424	0.942	0.216	0.364
m_1	1.846	2.178	2.032	1.265	2.742	2.485
m_2	2.937	2.736	2.794	1.842	2.946	2.693
Time (s)	0.4	0.4	0.41	0.4	0.44	0.44

The crack can be identified by different deformation level of electroluminescence imaging. If the image is in dimmer state then intensity is also low, thus cracks can be identified. In this work, a voltage of 0.7V was applied to the panel and the EM emission was detected by a CCD camera, 12 bits with resolution of 1300×1100 pixels. The tests were performed inside a darkroom and the obtained EM data is converted into I_t according to the method proposed by Fuyuki *et al.* [49].

For numerical modeling, the cell number 2 has a crack near the right edge of the cell between two busbars. The local electrical resistance of this cell is increasing and

it can be observed that the dimmer EM signal around the crack. The EM image of four cell of the PV panel is shown in Figure-12. Location of crack can be clearly differentiated by

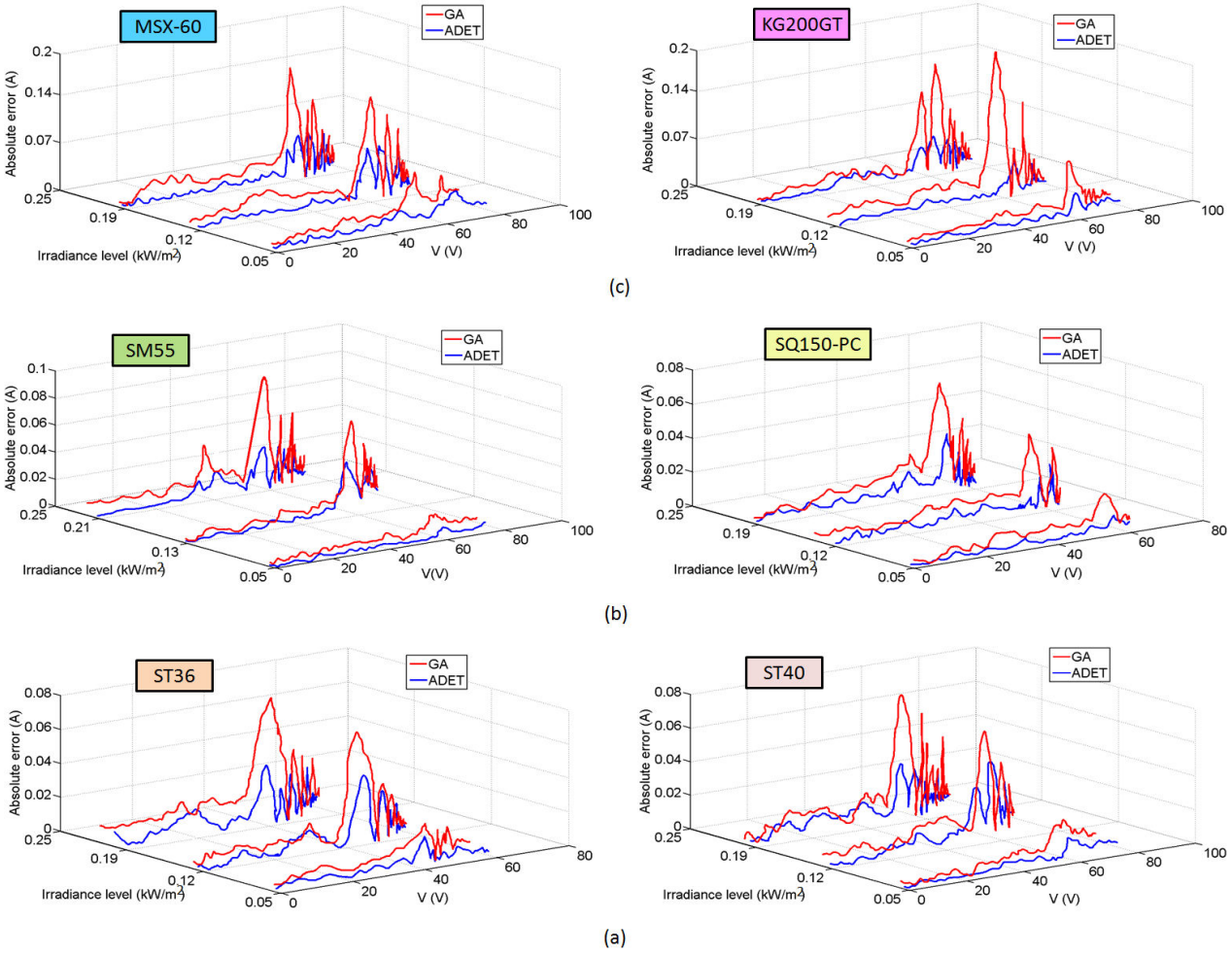

Figure-11. Absolute error for different irradiance levels (a) thin film (b) mono-crystalline (c) multi-crystalline.

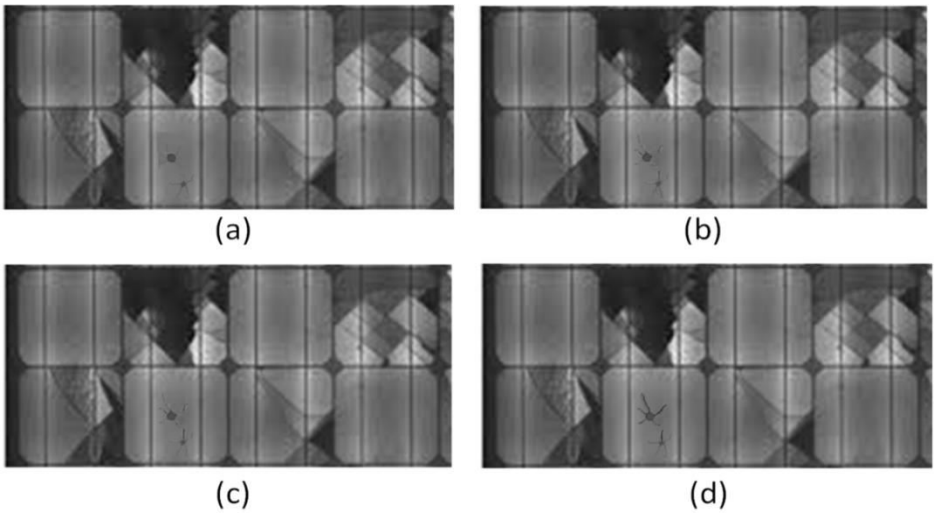

Figure-12. Electroluminescence image of the solar panel under different deflections (a) 4 cm, (b) 7 cm, (c) 10 cm, (d) 13 cm.

a circular spot on the center of mono-crystalline solar cell. This pattern cannot be identified by naked eye and only be determined by EM.

5. CONCLUSIONS

In this paper, a novel parameter extraction technique called ADET is used for solar cell modules. The proposed technique offers several advantages such as accuracy of solution, speed of convergence and balance between exploration and exploitation. The ADET method is applied to different types of solar cell modules such as thin film, mono-crystalline and multi-crystalline for five different irradiance of extracting the parameters. Comparisons are performed with other parameter extraction techniques such as CPSO, GA, SA, and OIS. Among these the proposed method performs better than other parameter extraction techniques. The feasibility of the ADET technique is verified by experimental V-I data set of thin film, mono-crystalline and multi-crystalline solar cell modules. Finally, the absolute error is computed for thin film, mono-crystalline and multi-crystalline solar cell modules for five different irradiance levels. It was found that the proposed technique is very accurate and rapid convergence to the solution. So the proposed method provides an alternate method to parameter extraction for solar cell models.

REFERENCES

[1] Golden JS, Carlson J, Kaloush KE, Phelan P, A comparative study of thermal and radiative impacts of photovoltaic canopies on pavement surface temperatures. Solar Energy 2007;81: 872-883.

[2] Nogueira CEC, Vidottob MI, Niedzialkoski RK, de Souza SNM, Chaves LI, Edwiges T, *et al*. Sizing and simulation of a photovoltaic-wind energy system sing batteries, applies for a small rural property located in the south of Brazil. Renewable and sustainable Energy Review 2014; 29:151-157.

[3] Bekele G, Palm B, Feasibility study for a standalone solar-wind based hybrid energy system for application in Ethiopia. Applied Energy 2010; 87:487-495.

[4] Bekele G, Palm B. Design of a photovoltaic-wind hybrid power generation system for Ethiopian remote area. Energy Proceedia 2012; 14:1760-1765.

[5] Fahmy FH, Ahmed NM, Farghally HM. Optimization of renewable energy power system for small scale brackish reverse osmosis desalination unit and a tourism motel in Egypt. Smart Grid Renewable Energy 2012; 3:43-50.

[6] Hafez O, Bhattacharya K. Optimal planning and design of a renewable energy based supply system for microgrids. Renewable Energy 2012; 45:7-15.

[7] G. Tina, A coupled electrical and thermal model for photovoltaic modules. J. Sol. Energy Eng. 2010; 132 (2):1–5.

[8] D. S. H. Chan and J. C. H. Phang, Analytical methods for the extraction of solar-cell single and double diode model parameters from I–V charac- teristics. IEEE Trans. Electron Devices 1987; 34(2):286–293.

[9] M.Hejri, H.Mokhtari, M.R.Azizian, and L.S¨oder, Ananalytical-numerical approach for parameter determination of a five parameter single-diode model of photovoltaic cells and modules. Int. J. Sus-tainableEnergy 2013. [Online].Available:http://dx.doi.org/10.1080/14786451. 2013.863886

[10] N. Enebish, D. Agchbayar, S. Dorjkhand, and D. Baatar, Numerical analysis of solar cell current-voltage characteristics. Sol. Energy Mater. Sol. Cells 1993; 29:201–208.

[11] Gottschalg R et. al, The influence of the measurement environment on the accuracy of the extraction of the physical parameters of solar cells, Meas Sci Technol 1999;10:796.

[12] Köntges M, Kunze I, Kajari-Schröder S, Breitenmoser X, Bjørneklett B. The risk of power loss in crystalline silicon based photovoltaic modules due to micro-cracks. Solar Energy Mater Solar Cells 2011; 95:1131–7.

[13] Sander M, Dietrich S, Pander M, Ebert M, Bagdahn J. Systematic investigation of cracks in encapsulated solar cells after mechanical loading. Solar Energy Mater Solar Cells 2013; 111: 82-9.

[14] Saleem H, Karmalkar H. An analytical method to extract the physical parameters of a solar cell from four points on the J-V curve. IEEE Electron Device Letter 2009; 30(4):349-352.

[15] Kim W, Choi W. A novel parameter extraction method for the one-diode solar cell model. Solar Energy 2010; 84(6):1008-1019.

[16] Ishaque K, Salam Z. An improved modeling method to determine the model parameters of photovoltaic

(PV) modules using differential evolution (DE). Sol Energy 2011; 85:2349-2359.

[17] Lingyun X, Lefei S, Wei H, Cong J. Solar cell parameter extraction using a hybrid genetic algorithm. In: Third International Conference on Measuring Technology and mechatronics automation; 2011; 306-309.

[18] Jervase JA *et al*. Solar cell parameter extraction using genetic algorithm. Meas Sci Technol 2001; 12:1922.

[19] Macabebe EQB, Sheppard CJ, Van Dyk EE. Parameter extraction from I-V characteristics of PV devices. Sol Energy 2011; 85:12-18.

[20] Asif S. Solar cell modeling and parameter optimization using simulated annealing. J. Propul Power 2008; 24:1018-22.

[21] Zagrouba M, Sellami A, Bouaicha M, Ksouri M. Identification of PV solar cells and modules parameters using the genetic algorithm: application to maximum power generation. Solar Energy 2010; 84(5):860-866.

[22] Ye M, Wang X, Xu Y. Parameter extraction of solar cells using particle swam optimization. J. Appl Phys 2009; 105(9):094502.

[23] Huang W, Jiang C, Xue L, Song D. Extracting solar cell model parameters based on chaos particle swam optimization. In: Proceedings of International Conference on Electric Information and Control Engineering (ICEICE) 2011; 398-402.

[24] Ishaque K, Salam Z, Mekhilef S, Shamsudin A. Parameter extraction of solar photovoltaic modules using penalty-based differential evolution. Appl. Energy 2012; 99: 297-308.

[25] Ji M, Jin Z, Tang H. An improved simulated annealing for solving the linear constrained optimization problems. Appl Math Comput 2006; 183:251-259.

[26] Ye M, Wang X, Xu Y. An extraction method of solar cell parameters with improved particle swam optimization. J. Appl. Phys 2009; 105:1099-104.

[27] Sandrolini L, Artioli M, Reggiani U. Numerical method for the extraction of photovoltaic module double-diode model parameters through cluster analysis. Appl Energy 2010; 87:442-51.

[28] Wang W, Wu J-M, Liu J-H, A particle swarm optimization based on chaotic neighborhood search to avoid premature convergence. In: Third international conference on genetic and evolutionary, computing 2009; 633-636.

[29] M. Chegaar, N. Nehaoua, A. Bouhemadou, Organic and inorganic solar cells parameters evauation from single I-V plot, Energy conversion and management 2008;49:1376-1379.

[30] El-Naggar. K.M, AlRashidi MR, AlHajri, Al-Othman A.K, Simulated annealing algorithm for photovoltaic parameters identification, Solar Energy 2012;86(1):266-274.

[31] Ishaque K, Salam Z, Taheri H. Simple, Fast and accurate two-diode model for photovoltaic modules. Solar Energy Mater Sol Cells 2011; 95:586-594.

[32] Basil Jacob, Karthik Balasubramanian, Thanikanti Sudhakar Babu, N Rajasekar, Parameter Extraction of Solar PV Double Diode Model Using Artificial Immune System, IEEE International Conference on Signal Processing, Informatics, Communication and Energy Systems , 2015;1 - 5.

[33] Tian H.M, Mancilla David F, Ellis K, Muljadi E, Jenkins P, A cell-to-module -to-array detailed model for photovoltaic panels. Sol. nergy Mater. Solar Cells 202; 86 (9):2695-2706.

[34] Ishaque K, Salam Z, Taheri H. A comprehensive MATLAB simulink PV system simulated with partial shading capability based on two-diode model. Solar Energy 2011; 85:2217-2227.

[35] M. T. Boyd, S. A. Klein, D. T. Reindl, and B. P. Dougherty, Evaluation and validation of equivalent circuit photovoltaic solar cell performance models. J. Sol. Energy Eng. 2011; 133(2):1–13.

[36] D. Sera, R. Teodorescu, and P. Rodriguez, PV panel model based on datasheet values. In Proc. IEEE Int. Symp. Ind. Electron 2007; 2392– 2396.

[37] W. D. Soto, S. A. Klein, and W. A. Beckman, Improvement and validation of a model for photovoltaic array performance. Sol. Energy 2006; 80(1):78–88.

[38] Ji Y-H, Kim J-G, Park S-H, Won C-Y, C-language based PV array simulation technique considering effects of partial shading. In IEEE International Conference on Industrial Technology (ICIT) 2009; 1-6.

[39] Breitenstein O, Rißland S. A two diode model regarding the distributed series resistance. Solar Energy Mater Solar Cell 2013; 110. 77-6.

[40] Berardone I, Corrado M, Paggi M. A generalized electric model for mono and polycrystalline silicon in the presence of cracks and random defects. Energy Proc 2014; 55:22-9.

[41] Paggi M, Corrado M, Rodriguez MA. A multi-physics and multi-scale numerical approach to microcracking and power-loss in photovoltaic modules. Compos Struct 2013; 95:630-8.

[42] Storn R, Price K. Differential evolution-a simple and efficient heuristic for global optimization over continuous spaces. J Global Optimiz 1997; 11:341-59.

[43] Price KV An introduction to differential evolution. In: Corne D, Dorigo M, Glover M, editor. New ideas in optimization. London: McGraw-Hill; 1999; 79-108.

[44] Best J, Greiner S, Boskovic B, Mernik M, Zumer V. Self adapting control parameters in differential evolution: a comparative study in numerical benchmark problem. IEEE Transactions on Evolution Computation 2006; 10(6):646-657.

[45] Liu J, Lampinen J. A fuzzy adaptive differential evolution algorithm. Soft Computation 2005; 9(6):448-462.

[46] Zhang J, Sanderson A C, JADE: adaptive differential evolution with optional external archive. IEEE Transactions on Evolution Computation 2009; 13(5):945-958.

[47] Zhang J, Sanderson A C, Adaptive differential evolution: a robust approach to multimodal problem optimization. Springer-Verlag, Berlin. 2009.

[48] Mathews. J. H. (1987) Numerical Methods for Computer Science. Engineering and Mathematics. Prentice Hall, NJ.

[49] Fuyuki T, Kondo H, Kaji Y, Ogane A, Takahashi Y. Analytic findings in the electroluminescence characterization of crystalline silicon solar cells. J Appl Phys 2007; 101: 023711.